HHS Public Access

Author manuscript

Laryngoscope. Author manuscript; available in PMC 2021 January 01.

Published in final edited form as:

Laryngoscope. 2021 January ; 131(1): E259–E270. doi:10.1002/lary.28671.

Effects of Neurod1 Expression on Mouse and Human Schwannoma Cells

Jennifer Kersigo, MS[1,*], **Lintao Gu, MD**[2,5,*], **Linjing Xu, MS**[2,*], **Ning Pan, PhD**[1,4], **Sarath Vijayakuma, PhD**[3], **Timothy Jones, PhD**[3], **Seiji B. Shibata, MD, PhD**[2], **Bernd Fritzsch, PhD**[1,2], **Marlan R. Hansen, MD**[2]

[1]Department of Biology, University of Iowa, Iowa City, Iowa

[2]Department of Otolaryngology, University of Iowa, Iowa City, Iowa

[3]Department of Special Education & Communication Disorders, University of Nebraska, Lincoln, NE

[4]Decibel Pharmaceutical, Boston, MA

[5]Department of Otolaryngology, Qianfo Shan Hospital Affiliated to Shandong University, Jinan, Shandong, China

Abstract

Objective(s): The objective was to explore the effect of the proneuronal transcription factor Neurod1 on Schwann cell and schwannoma cell proliferation.

Methods: Using a variety of transgenic mouse lines we investigated how expression of Neurod1 affects medulloblastoma (MB) growth, schwannoma tumor progression, vestibular function, and Schwann cell (SC) proliferation. Primary human vestibular schwannoma (VS) cell cultures were transduced with adenoviral vectors expressing *Neurod1*. Cell proliferation was assessed by EdU uptake.

Results: Expression of Neurod1 reduced the growth of slow growing, but not fast growing, MB models. Gene transfer of *Neurod1* in human schwannoma cultures significantly reduced cell proliferation in dose dependent way. Deletion of the *Nf2* tumor suppressor gene via cre expression in SCs led to increased intraganglionic SC proliferation and mildly reduced Vestibular sensory-evoked potentials (VsEP) responses compared to age-matched wild-type littermates. The effect of Neurod1 induced expression on intraganglionic SC proliferation in animals lacking *Nf2* was mild and highly variable. Sciatic nerve axotomy significantly increased SC proliferation in wild-type and *Nf2*-null animals and expression of Neurod1 reduced the proliferative capacity of both wild-type and *Nf2*-null SCs following nerve injury.

Conclusions: Expression of Neurod1 reduces slow growing MB progression and reduces human schwannoma cell proliferation in primary VS cultures. In a genetic mouse model of schwannomas

Corresponding author: Marlan R Hansen, MD, Departments of Otolaryngology-Head and Neck Surgery and Neurosurgery, University of Iowa, Iowa City, IA 52242, Office: (319) 353-7151, Fax: (319) 356-4547, marlan-hansen@uiowa.edu.
*indicates equal contribution

Level of Evidence: not applicable

we find some effects of Neurod1 expression but the high variability indicates that more tightly regulated Neurod1 expression levels that mimic our *in vitro* data are needed to fully validate Neurod1 effects on schwannoma progression.

Keywords

vestibular schwannoma; Schwann cell; Neurod1; medulloblastoma; tumor suppression

Introduction:

Schwannomas arise from Schwann cells (SCs), especially those within sensory ganglia.[1] Mutation in the *NF2* tumor suppressor gene results in neurofibromatosis type 2 (NF2) leading to multiple intracranial and spinal neoplasms including bilateral vestibular schwannomas (VSs).[2–4] The inner ear connects to the brain via neurons of Scarpa's and spiral ganglia[5,6] associated with neural crest-derived SCs.[7] Neurons are postmitotic in early embryos[8] whereas SCs continue to proliferate.[9] Schwannomas most commonly affect the vestibular nerve indicating that Scarpa's ganglion SCs are particularly prone to neoplasia.[1,10]

Treatment of VSs with surgery or radiation often results in loss of vestibular, auditory, and, in some cases, facial nerve function.[11,12] Development of pharmacologic or molecular therapies to slow VS growth offers the potential to delay or even prevent loss of inner ear and facial nerve function; interventions particularly relevant for NF2 patients who typically suffer complete deafness and eventually succumb to overwhelming tumor burden. Several attempts using various pharmacological approaches are under way but none have proven effective in the long-term.[13]

Neurod1 is proneural basic Helix-loop-Helix (bHLH) gene with capacity to reprogram ectodermal cells into neurons.[14] *Neurod1* is essential for differentiation of inner ear neurons,[15] enteroendocrine cells in the intestine,[16] and of beta cells in the pancreas.[17,18] Neurod1 drives this differentiation in part through suppression of alternate cell fates.[5,19,20] Neurod1 also drives glia cells in the brain and spinal cord toward neuronal differentiation.[21,22] Further, Neurod1 directs conversion of ear associated non-neuronal cells into neurons *in vitro*.[23] Beyond differentiation, Neurod1 also affects cell cycle illustrated in the cerebellum where Neurod1 overexpression forces cell cycle exit,[24] whereas absence of Neurod1 results in additional proliferation.[25] Neurod1 induces cell cycle arrest in part by increasing expression of p21, an inhibitor of cyclin-dependent kinases,[26] and regulation, directly or indirectly, of about 3000 genes.[27]

Here we explore the ability of Neurod1 to reduce the growth potential of schwannoma cells. Using viral-mediated gene transfer we show that Neurod1 reduces human VS cell proliferation *in vitro*. To further explore the ability of Neurod1 to suppress neural based neoplasms *in vivo*, we crossed a transgenic mouse line that expresses Neurod1 upon cre mediated recombination of floxed stop codon[19,28] into two different mouse lines that form cre induced medulloblastoma (MB).[29] We found a reduction of tumor progression in faster growing MB following cre-mediated *Neurod1* expression. We then crossed the cre induced *Neurod1* expressing mice with the SC-specific *Periostin-cre* mouse line that recombines

floxed *Nf2* (Postn-cre; $Nf2^{flox/flox}$) to reliably produce schwannomas in multiple cranial and spinal nerves, including the vestibular nerves.[30] The data suggest that Neurod1 expression could delay schwannoma growth but also show that additional manipulations of Neurod1 expression is necessary to develop an effective therapeutic approach to combat this late forming and slow growing tumor.

Material and Methods:

Mouse lines:

Periostin-cre (*Postn-cre*) were crossed with floxed *Nf2* gene (*Postn-cre;*$Nf2^{f/f}$) as previously described.[30] In addition, the *Postn-cre;*$Nf2^{f/f}$ mice were crossed with a $Rosa26^{LSL\text{-}Neurod1}$ ($R26^{ND1}$) line that induces Neurod1 expression via cre-mediated excision of a stop codon, enabling the Rosa26 locus to drive Neurod1 expression with or without elimination of the floxed *Nf2*. In addition we used the following mouse lines: tg(*Atoh1-cre)*;[8] $R26^{smo}$[29] and tg(*Neurod1-cre*)[16] to generate fast and slow growing medulloblastoma to assess the effect of Neurod1 expression on this neuronal tumor progression. In addition, we used the widely available $R26^{LacZ}$ reporter mice to verify that the Postn-cre effectively and exclusively recombines the stop codon in the Rosa26 locus. All procedures involving mice followed NIH guidelines and were approved by the University of Iowa animal care and use committee (IACUC protocol 7021971) and IRB approval (201205804) for human VS cells.

Mouse breeding:

Postn-cre; $Nf2^{f/f}$; Postn-cre; $Nf2^{f/f}$; $R26^{ND1}$: Mice were bred to obtain littermates having Postn-cre and floxed *Nf2* (*Postn-cre; *$Nf2^{f/f}$, *Nf2* conditional knock-out (cKO)) with or without induced expression of *Neurod1* (*Postn-cre; *$Nf2^{f/f}$*; *$R26^{ND1}$*, Nf2* cKO+ND1) (Supplemental Fig. 1). Littermates expressing *Neurod1* without deletion of *Nf2* were used to test the effect of *Neurod1* expression on SCs. Control animals either lacked the cre or had cre without the floxed genes. Animals were coded so that investigators performing tumor, cellular, and functional tests were blinded to the mouse genotype. Mice were sacrificed at the end of the 12–15 months period.

Atoh1-cre; $R26^{smo;ND1}$ & ND1-cre; $R26^{smo;ND1}$: To assess how fast growing tumors are affected by Neurod1 expression we bred two lines of mice using the *Atoh1-cre* that expresses cre in the proliferating external granule layer.[25,29] However, these very rapid growing tumors showed no noticeable effect of Neurod1 expression so we generated a second, slower growing tumor that regulates *smoothened* (smo) and Neurod1 expression in mostly postmitotic differentiating granule cells (Supplemental Fig. 2)

Measuring proliferation rate in mouse schwannoma:

Mice aged 10–15 months were injected with EdU 50mg/kg IP four times in a 24 hour period (0, 4, 8 and 24 hrs) and collected within 72 hrs. Mice were perfused with 4% paraformaldehyde and vestibular and facial (geniculate) ganglia were dissected and reacted as whole mounts for EdU following an existing protocol.[31] Specifically, EdU was detected in whole ganglion using the Click-It EdU kit per manufacturer's instructions (Life Technologies) and counterstained with DAPI to label nuclei. Ganglia were imaged on a SP5

Leica confocal microscope and the number of EdU-positive nuclei was quantified using the maximum projection of the z-stack. Dissected ganglia were also used to measure the ganglia volume using confocal stacks and the Amira software as previously described.[31] N=6 for each group.

Primary human VS cultures:

Human VS tumors were collected for primary cell culture as previously described.[32–34] After VS cells were cultured without passaging for 10 days, Adenovirus (Ad) CMVempty vector (EV) at 5×10^9 pfu/mL, AdCMVNeuroD1 at 2×10^9 pfu/mL, or AdCMVNeuroD1 at 5×10^9 pfu/mL (ViraQuest, Inc.) were applied to the culture medium for 72 hours as before.[33,35,36] Edu staining was performed using Click-it EdU Alexa Fluor 633 Image Kit (ThermoFisher C10340) as before.[37] The percentage of EdU-positive cells to S100-positive nuclei were counted by 20× microscopic fields using the cell counting feature of MetaMorph software package. Data are averaged from independent cultures derived three separate sporadic human VSs.

Western blot:

Western blots of protein extracts prepared from VS culture lysates were performed as before.[33,38] The primary antibodies used were anti-NeuroD1 (Abcam, ab109224) and anti-β-actin (Sigma, A5316) with horse-radish peroxidase linked secondary antibodies (Cell Singling, 7074S, 7076S). The blots were performed on cultures derived from three separate VSs.

Sciatic nerve axotomies and EdU uptake:

A total of 20 adult mice (2–16months) were used; 6 mice control mice, 4 mice with Postn-cre;$R26^{ND1}$ and 5 mice each of *Nf2* cKO and *Nf2* cKO+ND1 mice. Sciatic nerve axotomy and quantification of EdU uptake was performed as previously described.[37,39]

In situ hybridization and X-Gal reaction:

We used established protocols and probes as before to reveal the distribution of LacZ activation via *Postn-cre* and reveal the distribution of endogenous and induced *Neurod1* and of endogenous *Atoh1* expression.[19,25,28]

Gait analysis:

Gait was analyzed using the Noldus Cat-Walk XT system as before.[39,40]

Direct vestibular tests:

Vestibular sensory-evoked potentials (VsEPs) were collected from the vestibular nerve and central relays on anesthetized mice using methods described in detail elsewhere.[41–43] Investigators were blind to the genotype. Animals were anesthetized with a ketamine/xylazine mixture (18 mg/ml ketamine, 2 mg/ml xylazine; 5 to 10 μl/g intraperitoneally). VsEPs assess gravity receptor function using the metrics of response thresholds, amplitudes and latencies. Following testing, animals were perfused with 4% paraformaldehyde for further processing. At least six animals per genotype were tested and significance for any

differences was evaluated using one-way or multivariate analysis of variance (ANOVA or MANOVA).

Results

Neurod1 effects on human schwannoma:

To assess the ability of Neurod1 overexpression to reduce schwannoma growth, primary human VS cell cultures were transduced with AdCMVNeuroD1 (ND1) or AdCMVempty (EV) vector at two different concentrations. Transduction efficiency of VS cells with adenoviral vectors is ~85%.[33,35,36] Cell proliferation was assessed by EdU uptake (Fig. 1A–D). We verified dose dependent Neurod1 expression by western blot (Fig. 1E). The data show statistically significant and dose dependent reduction in EdU uptake in VS cells that express Neurod1 relative to those treated with EV. Thus, gene transfer with Neurod1 expressing viral vectors reduces human VS proliferation *in vitro*.

Next, we sought to evaluate long term effects of Neurod1 expression on glial based tumor growth and SC health over time.[30] We analyzed mice of various genotypes that develop either MB or schwannomas in terms of tumor growth, cell proliferation and vestibular physiology.

Medulloblastoma:

As a proof of principle we first evaluated if Neurod1 expression driven by the *R26*^{ND1} expresser can affect a fast growing, postnatal neural tumor, MB.[44] A model of MB was developed that uses the Atoh1-*cre* transgene[8] to recombine a floxed stop codon resulting in expression of constitutively active *smoothened (smo)* that reliably develop tumors. These tumors resemble the human sonic hedgehog (Shh)-dependent MB[29,45,46] by enhancing Shh-mediated proliferation.[47] Two bHLH transcription factors, Atoh1 and Neurod1, play essential roles in the proliferation and differentiation of granule cell precursors, the cellular source of MB. Atoh1 regulates Shh signaling in granule cell precursors in the external granule cell layer (EGL) and result in MB formation in the cerebellum.[48] Neurod1 acts downstream of Atoh1 but also downregulates Atoh1 via a negative feedback loop in both cerebellum and inner ear.[19,25,28] We first generated the *Atoh1-cre; R26*^{smo} with or without the R26^{ND1} expresser. We found that expression of a constitutively active smo triggered by an *Atoh1-cre* transgene induces massive MB growth;[8,29] there was no recognizable effect of Neurod1 on this fast-growing MB at P24 (Fig. 2A,B and data not shown).

Molecular work indicates that MB formation requires Atoh1.[48] We next investigated if reduction of Atoh1 can slow down tumor progression in the Atoh1-cre induced constitutive expression of smo. Compared to mice with two copies of *Atoh1* gene, mice with Atoh-1 haploinsufficiency indeed showed slower MB progression (Fig. 2C). Expression of *R26*^{ND1} only reduced overall size of the cerebellum and truncated sublobule formation in the Atoh1-cre mediated expression of Neurod1 on the background of Atoh1 haploinsufficiency (Fig. 2D). Overall, *R26*^{ND1} expression seemingly did not slow down much the tumor progression in the Atoh1 haploinsufficiency model (compare Fig. 2E,F). However, closer examination showed that in areas of delayed upregulation of Atoh1-cre expression such as lobe IX[25]

there was marked difference between littermates with and without *R26*^{ND1} expression: without Neurod1 much of the EGL had transformed into MB (Fig. 2E) whereas this did not happen in the presence of Atoh1-cre mediated upregulation of Neurod1 (Fig. 2F). These data suggest that delayed expression of smo in external granule cells might allow Neurod1 to achieve the desired effect of reducing tumor progression.

To capture external granule cells toward the end of their proliferative phase, we focused on Neurod1, a gene downstream of Atoh1 and necessary for granule cell differentiation including migration from the EGL into the internal granule layer.[25,49] We used a Neurod1-cre line[16] to induce expression of R26^{smo}. These mice developed MB of variable size, increasing in the anterior and posterior direction (Fig. 2), reflecting the variable Neurod1 effects in mutants along the vermis.[25,49] Comparing littermates with or without the R26^{ND1} we found that MB formation was completely suppressed by R26^{ND1} in the anterior lobes of the cerebellum and is at least reduced in the posterior lobes (Fig. 3A–C). Specifically, after constitutively active smoothened is expressed in granule cell precursors they may remain in the EGL that has variable thickness in different lobes (Fig. 3B). Littermates that express Neurod1 driven off the R26 locus have near normal anterior lobes with only limited retention of external granule cells (Fig. 3C–K). Only the most posterior lobes IX and X turn into obvious MBs with continued proliferation (Fig. 3I). Nevertheless, these mice demonstrated reduced MB formation in the most posterior lobes of the vermis (Fig. 3C) indicating that the R26^{ND1} model may only suffice to reduce slow growing tumors but not to stop fast growing tumors. These data on MB suggest that the R26^{ND1} construct could likewise be effective for slow growing tumors such a schwannoma[50] but fails to abolish fast growing tumors. Importantly, the level of expression of Neurod1 through the Rosa26 locus might not be so high as to cause reprogramming of SCs into neurons as has been achieved with Neurod1 *in vitro*23 and *in vivo* with glia cells.[22]

Schwann cell expressing cre lines:

Recently, it was shown that a newly generated Postn-cre line drives cre expression specifically and exclusively in SCs.[51] We first verified that this cre line effectively recombines the floxed stop codon in the Rosa26 locus by imaging the expression of LacZ using the beta-galactosidase [X-gal] reaction (Fig. 4).[52] Removing the LoxP stop codon using the Postn-cre line results in expression of the blue X-gal reaction product in all SCs of peripheral nerves already in embryos (Fig. 4). The X-gal reaction is an enzymatic enhancement of beta-galactosidase that does allow assessing presence of cre but not quantification of the expression level of cre. We next sought to see if Neurod1 expressed of the Postn-cre recombined Rosa26 locus can be imaged using conventional *in situ* hybridization.[19] To achieve this we compared the expression of Postn-cre with Neurod1 alone or in combination with R26^{ND1}. The data showed that the Rosa26 driven levels of cre can be detected with this approach and match the levels of expression of Neurod1 driven of the Rosa26 locus (Supplemental Fig. 3).

VsEP Measurements:

Generally, all animals had well formed VsEP responses. Vestibular thresholds were within the normal range for all groups (−4.5 to −13.5 dB re:1g/ms, Fig. 5A). There were no

differences in mean threshold across genotypes (Supplemental Table 1, Fig. 5A). In all groups, response amplitudes increased and latencies decreased systematically in a normal manner with increasing stimulus level. At the highest stimulus levels (+6 dB re:1g/ms) response latencies tended to be delayed in Nf2 cKO animals however the mean latencies of p1, n1 and p2 were significantly longer only for Nf2 cKO+ND1 compared to controls (Fig. 5B, Supplemental Table 1; MANOVA post hoc Bonferroni. p1: $p = 0.015$, n1: $p = 0.002$, p2: $p = 0.001$). The response latencies for Nf2 cKO and Nf2 cKO+ND1 animals were not significantly different. Response amplitudes were reduced compared to controls in Nf2 cKO but not Nf2 cKO+ND1 animals (Fig. 5C,D; MANOVA post hoc Bonferroni: p1-n1: $p = 0.015$; p2-n1: $p = 0.007$). In Nf2 cKO+ND1 the findings of prolonged latencies are consistent with altered activation timing and slowing of propagation of the compound action potential. Reduced amplitudes with minimal change in latency in Nf2 cKO animals may reflect reduced numbers of highly synchronized vestibular neurons responding to the transient stimulus. When data are normalized and stimulus expressed in dB above threshold (dB SL), the differences between control and Nf2 cKO animals in latency and amplitude became less important, although significantly lower amplitudes for p2-n1 persisted in the Nf2 cKO animals (Fig. 5E,F, Supplemental Table 2; MANOVA post hoc Bonferroni p2-n1 at 13 dB SL: $p = 0.032$). Indeed, latency shifts relative to control animals were no longer significant in the Nf2 cKO+ND1 group suggesting that peripheral vestibular sensitivity played a role in delaying response peaks in these animals (Fig. 5E, Supplemental Table 2). The persisting lower amplitudes in the Nf2 cKO group indicates that in those animals the dysfunction was more than a simple reduction in vestibular sensitivity (Fig. 5F). It is notable that at the highest stimulus levels above threshold there were significant differences in p1-n1 amplitudes between the two treatment groups (Fig. 5E,F; MANOVA, post hoc Bonferroni, $p = 0.04$). In summary, there is a statistically significant reduction in VsEP amplitudes in Nf2 cKO mice. This effect is somewhat rescued in Nf2 cKO+ND1 mice.

Cat walk:

Given that the physiological tests conducted thus far showed similar trends of Neurod1 expression to reduce the *Nf2* deletion effects, we next asked if gait analysis[40] could reveal a vestibular function deficit (Supplemental Fig. 4). While there was a trend towards higher irregularity of limb movement in the Nf2 cKO compared to control mice, these relatively minor differences did not reach significance due to wide interindividual variations (Supplemental Fig. 4). Expression of NeuroD1 in Nf2 cKO+ND1 did not impact *Nf2* deletion effects.

Assessment of proliferation in tumors:

Given that Neurod1 reduced MB formation and proliferation of human VS cells, we next compared EdU uptake and size of vestibular and geniculate ganglia of the various genotypes at 12 months (Fig. 6). We exposed mice to several treatments of EdU and assayed EdU incorporation in whole dissected ganglia using the Click-IT reaction.[53,54] Vestibular ganglia demonstrated nodules of flattened EdU-positive cells surrounding individual large ganglion cells (Fig. 6A–C); these nodules were more frequent in Nf2 cKO with or without Neurod1 expression. Within these nodules most of the EdU uptake occurred near the center (Fig. 6D–F), suggesting that proliferation is highest in those cells immediately adjacent to neurons.

These nodules were equally obvious in the geniculate ganglia (data not shown). Quantifying the EdU positive profiles showed significant increase in proliferation of Nf2 cKOs compared to control animals (Fig. 6G, H). There was significant variability in EdU-uptake in Nf2 cKO +ND1 mice (Fig. 6G); these differences were not statistically significant.

We next investigated the volume of vestibular and geniculate ganglia (Fig. 6, Supplemental Fig. 5). We found an unusual increase in pigment cells in the geniculate ganglion (Supplemental Fig. 5A–C) of Nf2 cKO and Nf2 cKO+ND1 mice suggesting possible a molecular change in cell fate of SCs to pigment cells as both derive from neural crest. As with proliferation, the volume assay showed the largest variation in vestibular ganglia from Nf2 cKO+ND1 mice (Fig. 6I). A similar trend was seen in the geniculate ganglion, but here Neurod1 expression showed an even larger volume increase and EdU positive profiles showed significant increase in proliferation of Nf2 cKOs compared to control animals (Supplemental Fig. 5D–F).

Although schwannomas show a predilection for sensory ganglia, the vast majority of SCs reside in peripheral nerves. To determine the effect of Neurod1 expression on proliferation of peripheral SCs, we performed sciatic nerve axotomies and compared EdU uptake 7 days after injury (Fig. 7). There was only a very small effect of *Nf2* deletion on normal SC proliferation in uncut nerves (Fig 7A–D). As expected, cut nerves showed a dramatic increase in SC proliferation (Fig. 7 E–H). Deletion of *Nf2* did not affect this strong proliferative response. However, compared with control and Nf2 cKO groups, the percentage of EdU positive cells in Nf2cKO+ND1 group was significantly reduced ($p<0.05$) (Fig. 7I). Thus, expression of Neurod1 decreased SC proliferation following axotomy whether or not *Nf2* was also deleted.

Discussion

The main outcomes of our study are:

1. Expression of Neurod1 through the Rosa26 locus reduces but does not completely arrest slow growing MB tumors.
2. Viral mediated gene transfer of Neurod1 in primary human VS cultures significantly reduced cell proliferation.
3. Expression of Neurod1 had variable effects on schwannoma cell proliferation in animals lacking *Nf2*.
4. Neurod1 expression suppressed proliferation of wild-type and Nf2 cKO SCs following axotomy.

Medulloblastoma:

MBs account for ~30% of child brain tumors.[44] MB is primarily driven by a Shh activation of the already high proliferation rate in the external granule layer.[46,55] The external granule layer requires the presence of Atoh1 for proliferation as well as MB formation via the Shh signaling pathway.[48] We show that Neurod1, a factor downstream of Atoh1 that downregulates Atoh1 expression can affect MB progression but only in late proliferating

granule cells using the Atoh1-cre transgene (Fig. 2). However, using a novel MB model driven by the Neurod1-cre mediated late expression of smo that grows much slower compared to the Atoh1-cre mediated tumor,[29] we show noticeable reduction but not complete arrest in tumor progression by Neurod1 (Fig. 3). These data are consistent with the idea that certain slowly progressing neuronal tumors could be treatable with Neurod1 expression.

Schwannoma:

Germline damaging mutation in the *NF2* gene results in the NF2 syndrome characterized by multiple cranial and spinal schwannomas. Sporadic schwannomas are also associated with somatic loss of *NF2* function. Interestingly, both NF2-associated and sporadic schwannomas occur most commonly in sensory ganglia, particularly the vestibular ganglia, rather than along peripheral nerves.[1] A similar pattern of sensory ganglia SC tumors occurs in Postn-cre;$Nf2^{f/f}$ mice.[30] In this case, the increased cell growth occurs as tumorlets in which there are multiple small foci of aberrant cell growth throughout the ganglion (Fig. 6).[30] EdU uptake studies here demonstrated that the SCs surrounding the sensory neurons (i.e. satellite cells) are those that appear to be the most proliferative and contribute to tumorlet formation. There was little to no EdU uptake in similar satellite cells in control mice. These observations raise the possibility of a paracrine influence of the sensory neurons on SCs proliferation in the context of lost *Nf2* function that may account, at least in part, for the predisposition for schwannomas to form in sensory ganglia compared to peripheral nerves. Neurons of the inner ear have been shown to express neuregulin-1 (NRG-1) which serves as an ErbB2/3 ligand to promote SC proliferation.[56,57] Notably, human VSs also secrete NRG-1 providing an autocrine loop and neuron autonomous proliferation.[32,57]

Building on the insights gained from the MB analysis we show that variable levels of Neurod1 expression can indeed reduce human VS proliferation *in vitro* (Fig. 1). However, using the same mouse line that affects slower growing MB progression we only found mild and highly variable effects of Neurod1 expression on schwannoma proliferation in vestibular and geniculate ganglia (Fig. 6).

VsEP:

The deficits reflected by the VsEP in Nf2 cKO animals were modest. The absence of significant balance behavioral abnormalities in the Nf2 cKO animals reported here is not surprising given the modest nature of the vestibular deficit seen with the VsEP. Behavioral tests alone may not be sensitive to vestibular abnormalities (even severe deficits) owing to central compensation.[58] The VsEP measures vestibular neural responses to transient head motion that are mediated by irregularly discharging vestibular neurons.[59] As such the VsEP is less sensitive to responses to static or slowly changing head movements, which are mediated by different regularly discharging vestibular neurons. Moreover, the VsEP does not evaluate canal function. It’s possible therefore that other more serious functional deficits may be present in Nf2 deficient, which are not revealed by VsEPs.

Translational/clinical impact:

Current treatment strategies for schwannomas are limited to microsurgical removal or radiation, both of which carry significant risks to hearing, balance, and facial function.[11,12] Patients with NF2 are in particular need of effective alternative treatments to delay or prevent tumor growth. While there have been recent attempts to identify effective chemotherapies that target NF2 sensitive targets, most have failed to yield a clinical response and none have produced a durable response.[60–62] These results highlight the fact that targeting a single aberrant signaling pathway in schwannomas is unlikely to achieve a durable response. Here we tested a molecular approach to drive schwannoma cells out of the cell cycle. The level of Neurod1 expressed via the Rosa26 locus may have variable penetrance that is reflected in interindividual differences in cell proliferation. Indeed, the one clear effect of the complex gene interactions we tested here was a large variability at all levels. Based on the suppression of slower growing MB with Neurod1 together with the dose-dependent effect of Neurod1 on human schwannoma proliferation, we suggest that constructs with a highly regulated level of Neurod1 expression are needed to move this approach forward. Future therapies could rely on viral vectors carrying artificial enhancer element driven constructs that allow defined levels of Neurod1 expression specifically in schwannoma cells.[63]

Conclusions

In conclusion, expression of Neurod1 reduces proliferation of both control and *Nf2* deficient SCs following nerve injury and indicates that tightly regulated Neurod1 overexpression could be developed into a therapeutic approach to delay schwannoma growth.

Supplementary Material

Refer to Web version on PubMed Central for supplementary material.

Acknowledgements:

The authors acknowledge the support of Drs. Andrew Leiter and Joyce Li for providing the Rosa26^{ND1} expressing mice.

Funding and Conflict of Interests: This work was supported by grants from the Carver College of Medicine, NCATS UL1TR002537, and R01 AG060504.

References:

1. Tryggvason G, Barnett A, Kim J, Soken H, Maley J, Hansen MR. Radiographic association of schwannomas with sensory ganglia. Otology & Neurotology 2012; 33:1276–1282. [PubMed: 22858714]
2. Rouleau GA, Merel P, Lutchman Met al. Alteration in a new gene encoding a putative membrane-organizing protein causes neuro-fibromatosis type 2. Nature 1993; 363:515–521. [PubMed: 8379998]
3. Trofatter JA, MacCollin MM, Rutter JLet al. A novel moesin-, ezrin-, radixin-like gene is a candidate for the neurofibromatosis 2 tumor suppressor. Cell 1993; 72:791–800. [PubMed: 8453669]
4. Evans DG. Neurofibromatosis type 2 (NF2): a clinical and molecular review. Orphanet J Rare Dis 2009; 4:16. [PubMed: 19545378]

5. Macova I, Pysanenko K, Chumak Tet al. Neurod1 Is Essential for the Primary Tonotopic Organization and Related Auditory Information Processing in the Midbrain. J Neurosci 2019; 39:984–1004. [PubMed: 30541910]
6. Rubel EW, Fritzsch B. Auditory system development: primary auditory neurons and their targets. Annu Rev Neurosci 2002; 25:51–101. [PubMed: 12052904]
7. Mao Y, Reiprich S, Wegner M, Fritzsch B. Targeted deletion of Sox10 by Wnt1-cre defects neuronal migration and projection in the mouse inner ear. PLoS One 2014; 9:e94580. [PubMed: 24718611]
8. Matei V, Pauley S, Kaing Set al. Smaller inner ear sensory epithelia in Neurog 1 null mice are related to earlier hair cell cycle exit. Dev Dyn 2005; 234:633–650. [PubMed: 16145671]
9. Tomasetti C, Vogelstein B. Cancer etiology. Variation in cancer risk among tissues can be explained by the number of stem cell divisions. Science 2015; 347:78–81. [PubMed: 25554788]
10. Cutfield SW, Wickremesekera AC, Mantamadiotis Tet al. Tumour stem cells in schwannoma: A review. J Clin Neurosci 2019; 62:21–26. [PubMed: 30626543]
11. Monfared A, Corrales CE, Theodosopoulos PVet al. Facial Nerve Outcome and Tumor Control Rate as a Function of Degree of Resection in Treatment of Large Acoustic Neuromas: Preliminary Report of the Acoustic Neuroma Subtotal Resection Study (ANSRS). Neurosurgery 2016; 79:194–203. [PubMed: 26645964]
12. Meyer TA, Canty PA, Wilkinson EP, Hansen MR, Rubinstein JT, Gantz BJ. Small acoustic neuromas: surgical outcomes versus observation or radiation. Otology & Neurotology 2006; 27:380–392. [PubMed: 16639278]
13. Plotkin SR, Albers AC, Babovic-Vuksanovic Det al. Update from the 2013 International Neurofibromatosis Conference. American journal of medical genetics Part A 2014; 164A:2969–2978. [PubMed: 25255738]
14. Lee JE, Hollenberg SM, Snider L, Turner DL, Lipnick N, Weintraub H. Conversion of Xenopus ectoderm into neurons by NeuroD, a basic helix-loop-helix protein. Science 1995; 268:836–844. [PubMed: 7754368]
15. Kim WY, Fritzsch B, Serls Aet al. NeuroD-null mice are deaf due to a severe loss of the inner ear sensory neurons during development. Development 2001; 128:417–426. [PubMed: 11152640]
16. Li HJ, Kapoor A, Giel-Moloney M, Rindi G, Leiter AB. Notch signaling differentially regulates the cell fate of early endocrine precursor cells and their maturing descendants in the mouse pancreas and intestine. Developmental biology 2012; 371:156–169. [PubMed: 22964416]
17. Naya FJ, Huang HP, Qiu Yet al. Diabetes, defective pancreatic morphogenesis, and abnormal enteroendocrine differentiation in BETA2/neuroD-deficient mice. Genes Dev 1997; 11:2323–2334. [PubMed: 9308961]
18. Gu C, Stein GH, Pan Net al. Pancreatic beta cells require NeuroD to achieve and maintain functional maturity. Cell Metab 2010; 11:298–310. [PubMed: 20374962]
19. Jahan I, Pan N, Kersigo J, Fritzsch B. Neurod1 suppresses hair cell differentiation in ear ganglia and regulates hair cell subtype development in the cochlea. PLoS One 2010; 5:e11661. [PubMed: 20661473]
20. Li HJ, Ray SK, Singh NK, Johnston B, Leiter AB. Basic helix-loop-helix transcription factors and enteroendocrine cell differentiation. Diabetes Obes Metab 2011; 13 Suppl 1:5–12. [PubMed: 21824251]
21. Guo Z, Zhang L, Wu Z, Chen Y, Wang F, Chen G. In vivo direct reprogramming of reactive glial cells into functional neurons after brain injury and in an Alzheimer's disease model. Cell stem cell 2014; 14:188–202. [PubMed: 24360883]
22. Chen W, Zhang B, Xu S, Lin R, Wang W. Lentivirus carrying the NeuroD1 gene promotes the conversion from glial cells into neurons in a spinal cord injury model. Brain Res Bull 2017; 135:143–148. [PubMed: 28987284]
23. Noda T, Meas SJ, Nogami Jet al. Direct Reprogramming of Spiral Ganglion Non-neuronal Cells into Neurons: Toward Ameliorating Sensorineural Hearing Loss by Gene Therapy. Front Cell Dev Biol 2018; 6:16. [PubMed: 29492404]
24. Butts T, Hanzel M, Wingate RJ. Transit amplification in the amniote cerebellum evolved via a heterochronic shift in NeuroD1 expression. Development 2014; 141:2791–2795. [PubMed: 25005474]

25. Pan N, Jahan I, Lee JE, Fritzsch B. Defects in the cerebella of conditional Neurod1 null mice correlate with effective Tg(Atoh1-cre) recombination and granule cell requirements for Neurod1 for differentiation. Cell and tissue research 2009; 337:407–428. [PubMed: 19609565]
26. Mutoh H, Naya FJ, Tsai MJ, Leiter AB. The basic helix-loop-helix protein BETA2 interacts with p300 to coordinate differentiation of secretin-expressing enteroendocrine cells. Genes Dev 1998; 12:820–830. [PubMed: 9512516]
27. Pataskar A, Jung J, Smialowski Pet al. NeuroD1 reprograms chromatin and transcription factor landscapes to induce the neuronal program. EMBO J 2016; 35:24–45. [PubMed: 26516211]
28. Jahan I, Kersigo J, Pan N, Fritzsch B. Neurod1 regulates survival and formation of connections in mouse ear and brain. Cell and tissue research 2010; 341:95–110. [PubMed: 20512592]
29. Schuller U, Heine VM, Mao Jet al. Acquisition of granule neuron precursor identity is a critical determinant of progenitor cell competence to form Shh-induced medulloblastoma. Cancer Cell 2008; 14:123–134. [PubMed: 18691547]
30. Gehlhausen JR, Park SJ, Hickox AEet al. A murine model of neurofibromatosis type 2 that accurately phenocopies human schwannoma formation. Human molecular genetics 2015; 24:1–8. [PubMed: 25113746]
31. Kopecky BJ, Duncan JS, Elliott KL, Fritzsch B. Three-dimensional reconstructions from optical sections of thick mouse inner ears using confocal microscopy. Journal of microscopy 2012; 248:292–298. [PubMed: 23140378]
32. Hansen MR, Roehm PC, Chatterjee P, Green SH. Constitutive neuregulin-1/ErbB signaling contributes to human vestibular schwannoma proliferation. Glia 2006; 53:593–600. [PubMed: 16432850]
33. Yue WY, Clark JJ, Fernando A, Domann F, Hansen MR. Contribution of persistent C-Jun N-terminal kinase activity to the survival of human vestibular schwannoma cells by suppression of accumulation of mitochondrial superoxides. Neuro-oncology 2011; 13:961–973. [PubMed: 21697181]
34. Schularick NM, Clark JJ, Hansen MR. Primary culture of human vestibular schwannomas. Journal of visualized experiments : JoVE 2014.
35. Ahmad I, Yue WY, Fernando A, Clark JJ, Woodson EA, Hansen MR. p75NTR is highly expressed in vestibular schwannomas and promotes cell survival by activating nuclear transcription factor kappaB. Glia 2014; 62:1699–1712. [PubMed: 24976126]
36. Yue WY, Clark JJ, Telisak M, Hansen MR. Inhibition of c-Jun N-terminal kinase activity enhances vestibular schwannoma cell sensitivity to gamma irradiation. Neurosurgery 2013; 73:506–516. [PubMed: 23728448]
37. Ahmad I, Fernando A, Gurgel R, Jason Clark J, Xu L, Hansen MR. Merlin status regulates p75 expression and apoptotic signaling in Schwann cells following nerve injury. Neurobiol Dis 2015; 82:114–122. [PubMed: 26057084]
38. Brown KD, Hansen MR. Lipid raft localization of erbB2 in vestibular schwannoma and Schwann cells. Otology & Neurotology 2008; 29:79–85. [PubMed: 18199961]
39. Truong K, Ahmad I, Jason Clark Jet al. Nf2 Mutation in Schwann Cells Delays Functional Neural Recovery Following Injury. Neuroscience 2018; 374:205–213. [PubMed: 29408605]
40. Kopecky B, Decook R, Fritzsch B. Mutational ataxia resulting from abnormal vestibular acquisition and processing is partially compensated for. Behavioral neuroscience 2012; 126:301–313. [PubMed: 22309445]
41. Jones SM, Erway LC, Bergstrom RA, Schimenti JC, Jones TA. Vestibular responses to linear acceleration are absent in otoconia-deficient C57BL/6JEi-het mice. Hear Res 1999; 135:56–60. [PubMed: 10491954]
42. Jones SM, Jones TA, Johnson KR, Yu H, Erway LC, Zheng QY. A comparison of vestibular and auditory phenotypes in inbred mouse strains. Brain Res 2006; 1091:40–46. [PubMed: 16499890]
43. Vijayakumar S, Depreux FF, Jodelka FMet al. Rescue of peripheral vestibular function in Usher syndrome mice using a splice-switching antisense oligonucleotide. Human molecular genetics 2017; 26:3482–3494. [PubMed: 28633508]
44. Northcott PA, Korshunov A, Pfister SM, Taylor MD. The clinical implications of medulloblastoma subgroups. Nat Rev Neurol 2012; 8:340–351. [PubMed: 22565209]

45. Morrissy AS, Cavalli FMG, Remke Met al. Spatial heterogeneity in medulloblastoma. Nat Genet 2017; 49:780–788. [PubMed: 28394352]
46. Tan IL, Wojcinski A, Rallapalli Het al. Lateral cerebellum is preferentially sensitive to high sonic hedgehog signaling and medulloblastoma formation. Proc Natl Acad Sci U S A 2018; 115:3392–3397. [PubMed: 29531057]
47. Zarei S, Zarei K, Fritzsch B, Elliott KL. Sonic hedgehog antagonists reduce size and alter patterning of the frog inner ear. Developmental neurobiology 2017; 77:1385–1400. [PubMed: 29030893]
48. Flora A, Klisch TJ, Schuster G, Zoghbi HY. Deletion of Atoh1 disrupts Sonic Hedgehog signaling in the developing cerebellum and prevents medulloblastoma. Science 2009; 326:1424–1427. [PubMed: 19965762]
49. Miyata T, Maeda T, Lee JE. NeuroD is required for differentiation of the granule cells in the cerebellum and hippocampus. Genes Dev 1999; 13:1647–1652. [PubMed: 10398678]
50. Stangerup SE, Caye-Thomasen P, Tos M, Thomsen J. The natural history of vestibular schwannoma. Otology & Neurotology 2006; 27:547–552.
51. Lindsley A, Snider P, Zhou Het al. Identification and characterization of a novel Schwann and outflow tract endocardial cushion lineage-restricted periostin enhancer. Developmental biology 2007; 307:340–355. [PubMed: 17540359]
52. Matei VA, Feng F, Pauley S, Beisel KW, Nichols MG, Fritzsch B. Near-infrared laser illumination transforms the fluorescence absorbing X-Gal reaction product BCI into a transparent, yet brightly fluorescent substance. Brain Res Bull 2006; 70:33–43. [PubMed: 16750480]
53. Buck SB, Bradford J, Gee KR, Agnew BJ, Clarke ST, Salic A. Detection of S-phase cell cycle progression using 5-ethynyl-2'-deoxyuridine incorporation with click chemistry, an alternative to using 5-bromo-2'-deoxyuridine antibodies. Biotechniques 2008; 44:927–929. [PubMed: 18533904]
54. Zeng C, Pan F, Jones LAet al. Evaluation of 5-ethynyl-2'-deoxyuridine staining as a sensitive and reliable method for studying cell proliferation in the adult nervous system. Brain Res 2010; 1319:21–32. [PubMed: 20064490]
55. Jones DT, Jager N, Kool Met al. Dissecting the genomic complexity underlying medulloblastoma. Nature 2012; 488:100–105. [PubMed: 22832583]
56. Hansen MR, Vijapurkar U, Koland JG, Green SH. Reciprocal signaling between spiral ganglion neurons and Schwann cells involves neuregulin and neurotrophins. Hear Res 2001; 161:87–98. [PubMed: 11744285]
57. Hansen MR, Linthicum FH Jr Expression of neuregulin and activation of erbB receptors in vestibular schwannomas: possible autocrine loop stimulation. Otology & Neurotology 2004; 25:155–159. [PubMed: 15021776]
58. Mathur PD, Vijayakumar S, Vashist D, Jones SM, Jones TA, Yang J. A study of whirlin isoforms in the mouse vestibular system suggests potential vestibular dysfunction in DFNB31-deficient patients. Human molecular genetics 2015; 24:7017–7030. [PubMed: 26420843]
59. Lee C, Holt JC, Jones TA. Effect of M-current modulation on mammalian vestibular responses to transient head motion. Journal of neurophysiology 2017; 118:2991–3006. [PubMed: 28855291]
60. Karajannis MA, Legault G, Hagiwara Met al. Phase II trial of lapatinib in adult and pediatric patients with neurofibromatosis type 2 and progressive vestibular schwannomas. Neuro-oncology 2012; 14:1163–1170. [PubMed: 22844108]
61. Karajannis MA, Legault G, Hagiwara Met al. Phase II study of everolimus in children and adults with neurofibromatosis type 2 and progressive vestibular schwannomas. Neuro-oncology 2014; 16:292–297. [PubMed: 24311643]
62. Blakeley JO, Plotkin SR. Therapeutic advances for the tumors associated with neurofibromatosis type 1, type 2, and schwannomatosis. Neuro-oncology 2016; 18:624–638. [PubMed: 26851632]
63. Xie M, Fussenegger M. Designing cell function: assembly of synthetic gene circuits for cell biology applications. Nat Rev Mol Cell Biol 2018; 19:507–525. [PubMed: 29858606]

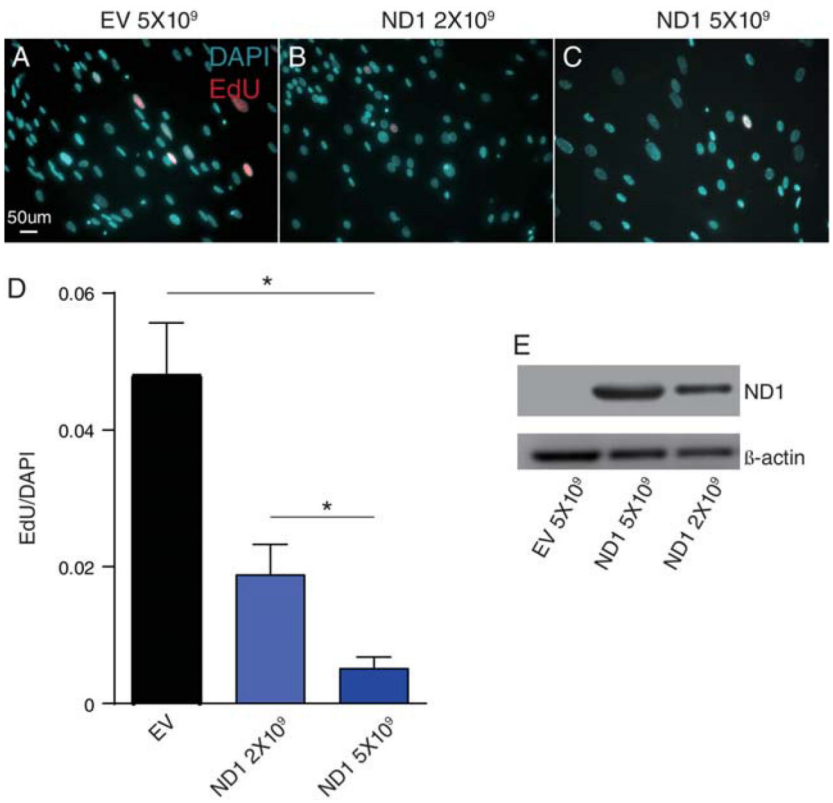

Figure 1.

Effect of Neurod1 expression on human vestibular schwannoma (VS) cells *in vitro*. Primary human VS cultures were treated with empty vector (EV) or vectors of different concentration carrying Neurod1. (A) Western blot of lysates from VS cultures treated with adenovirus expressing ND1 (2×10^9 or 5×10^9 pfu/ml) or empty vector (EV, 5×10^9 pfu/ml) and probed with anti-ND1 antibodies followed by anti-β-actin antibodies. (B,C) Primary human VS cultures labeled with EdU. The percentage of EdU positive, S100-positive nuclei to total S100-positive nuclei were counted by 20× microscopic fields and are expressed here as numbers of EdU positive nuclei per DAPI stained nuclei. Cultures treated with 5×10^9 EV showed significantly more EdU incorporation (***$p<0.05$) compared to either 2×10^9 or 5×10^9 ND1 containing vectors.

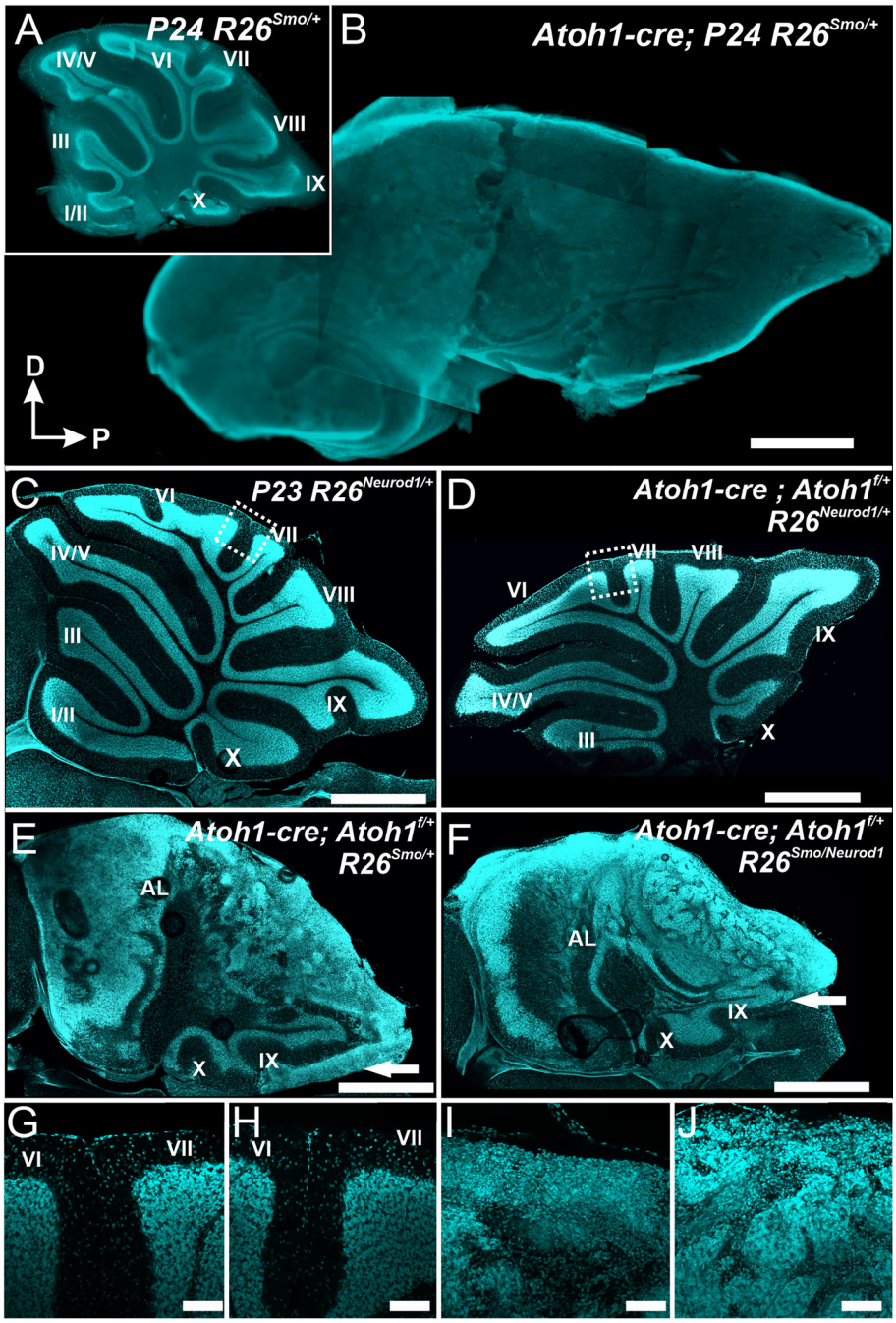

Figure 2.

Atoh1-cre induced overexpression of smoothened (smo) results in a rapid growth of MB (B) in mice. Control littermates have a drastically smaller and highly differentiated cerebellum (A). The size of the MB in mice expressing Neurod1 (F) was indistinguishable from simple smoothened overexpresser, indicating that Neurod1 expressed off the Rosa26 locus does not suffice to alter the fate after Atoh1-cre induced constitutively active smo. Reducing the Atoh1 level in combination with expression of Neurod1 from the Rosa26 locus has only minor effects on overall cerebellar development (note the reduction in lob size and in

particular loss of sublobes in D compared to C). Reducing Atoh1 while expressing constitutively active smo with (F) or without (E) Neurod1 causes slower MB formation through transformation of the embryonic external granular layer. However, this transformation extends only in mice without Neurod1 into lobes with late expression of the Atoh1-cre transgene (IX and X). Comparing lobe IX with or without Neurod1 (arrow in E,F) shows reduced transformation of external granular cell layer into MB. Details of central lobes show that overexpression of Neurod1 has no major defect (G, I) but affects tumor progression by allowing some external granular cells to variably migrate to the internal granular layer. Scale bars indicate 1mm in A-F and100 μm in G-J.

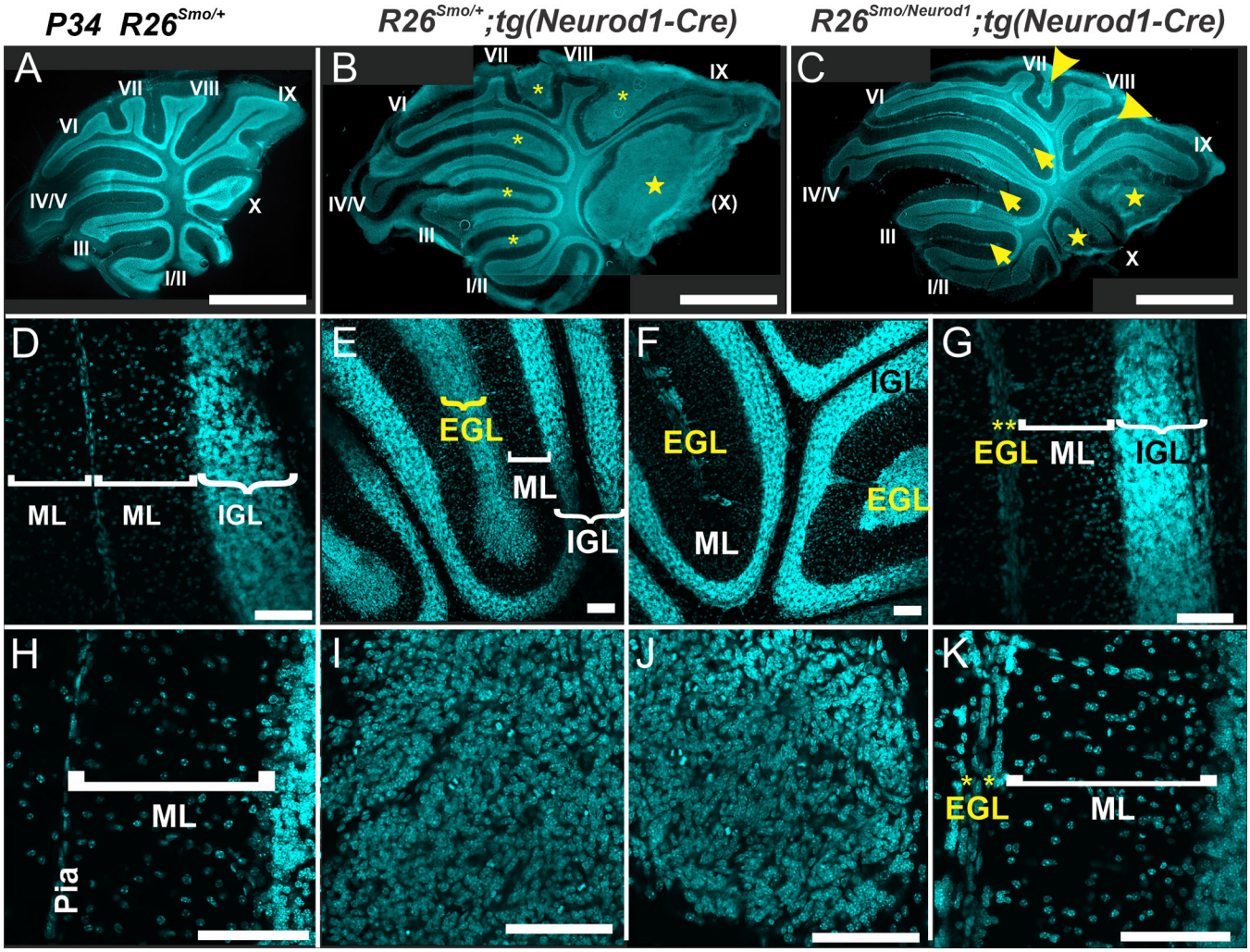

Figure 3.

Neurod1-Cre induced overexpression of constitutively active smo results in retention of a variable sized external granule layer (EGL) in each lobe (small * in B) and medulloblastoma (MB) formation in the posterior lobe (large * in B, lobe X) of the cerebellum. Higher magnification reveals that instead of molecular layers separated only by a thin layer of meninges (Pia in D,H) the EGL of adjacent folia merge (E). In lobes IX and X small MBs form that show abundant proliferation as demonstrated by numerous cell divisions (I). Overexpression of Neurod1 suppresses the formation of extra EGL and MB formation caused by smo overexpression, resulting in near normal EGL in anterior lobes (F, G, K, arrows in C) and reduced EGL in posterior lobes (arrow heads in C). Starting at lobe VII (C) there was a variable formation of MB (C, J) Scale bars= 1mm in A,B,C and 100 μm all other images.

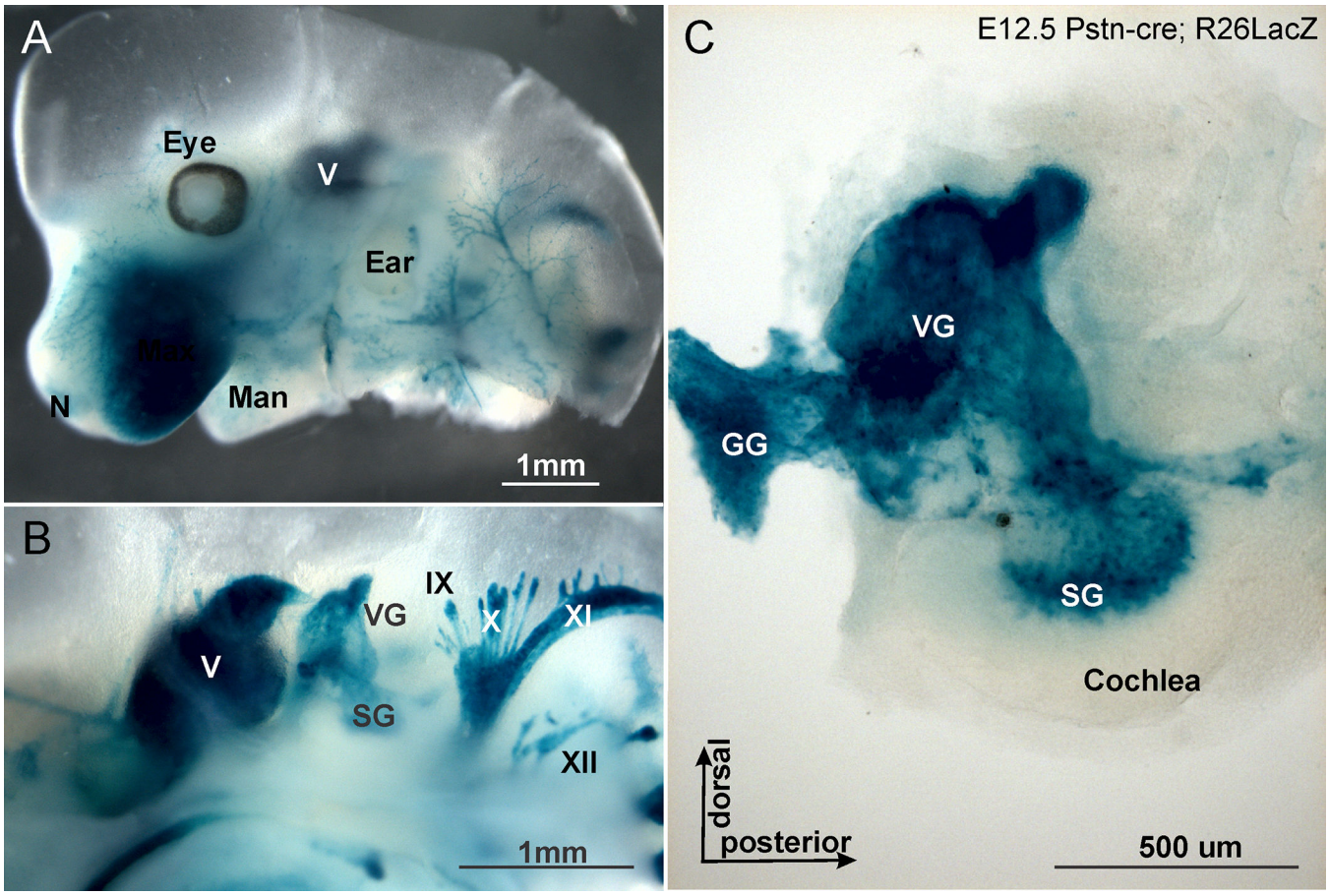

Figure 4.

X-gal staining using Rosa26 LacZ reporter reveals the distribution of beta-galactosidase after Postn-cre mediated recombination. Note that only peripheral SCs in mouse cranial nerves of this E12.5 day old mouse are positive. (A) Lateral view of the head with profound expression in nerves to various skin regions. (B) Medial view showing labeling in cranial ganglia and nerves. (C) Detail of the microdissected ear with X-gal stain in vestibular, geniculate and spiral ganglion. The same Rosa26 expression is expected after Postn-cre mediated recombination of the floxed stop codon in the $R26^{ND1}$ transgenic animal and will reflect the deletion of the floxed Nf2 gene after Postn-cre mediated recombination. Note absence of X-gal staining in the brain or ear (A,C). V, VII, X, XI, XII, corresponding cranial nerves. Scale bar=1 mm in A,B and 100 μm in C.

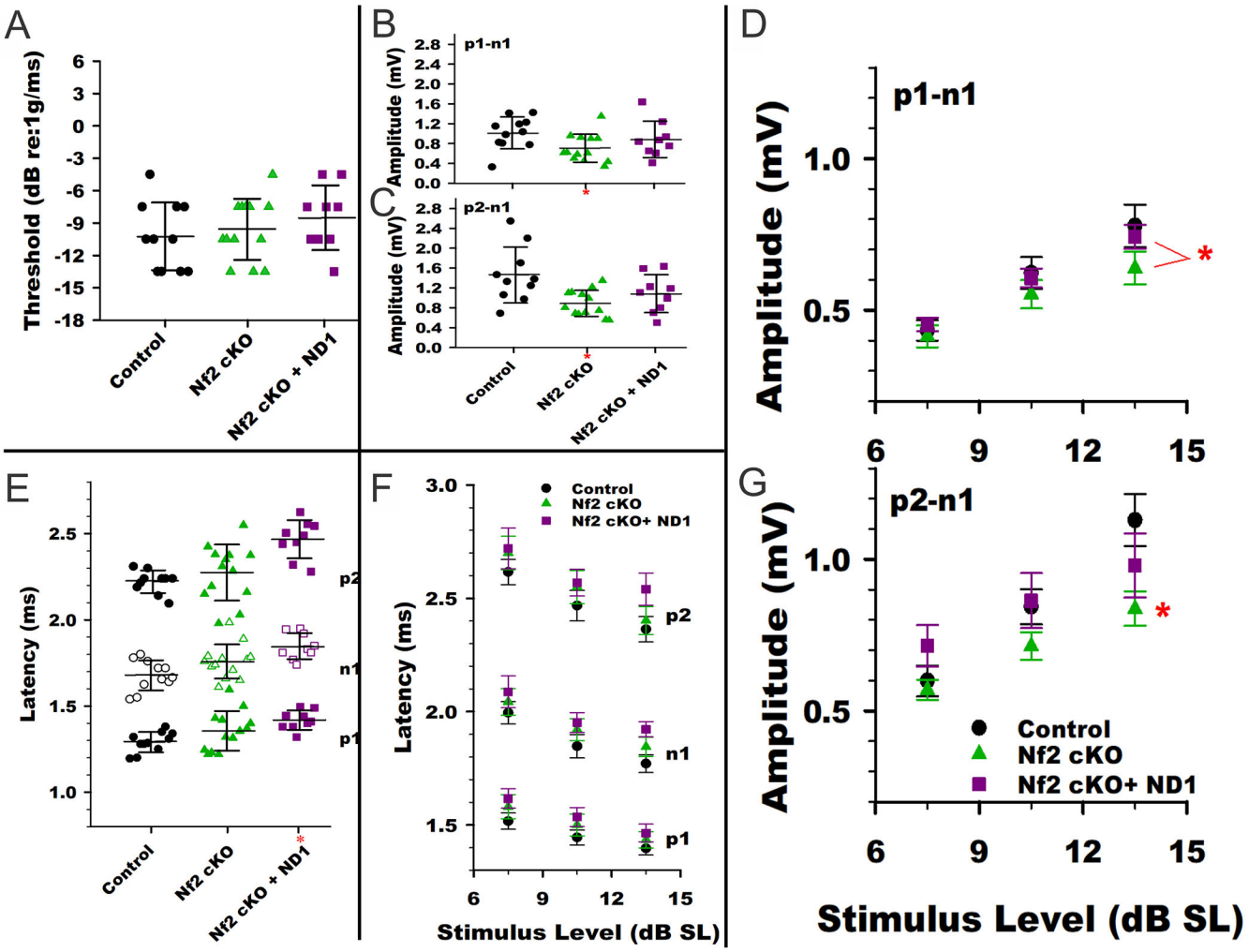

Figure 5.

VsEP responses for the three genotypes. (A) VsEP threshold distributions among the different genotypes. There were no significant differences in mean threshold across groups. (B) VsEP Latencies at +6dB re:1g/ms. Latency distributions across animals are plotted for the three genotypes. Latencies (p1, n1 & p2) on average for the KO+ND1 group were prolonged relative to the control group (MANOVA post hoc Bonf. p1: p = 0.015, n1: p = 0.002, p2: p = 0.001). Dashed red line reflect the mean latencies for the control group. (C,D) VsEP Amplitudes at a stimulus level of +6 dB re:1g/ms. Mean amplitude for KO animals (*) were reduced compared to the control group (MANOVA post hoc Bonf: p1-n1: p = 0.015; p2-n1: p = 0.007). Mean amplitude for the KO+ND1 group was not significantly different than controls. (E) Normalized VsEP latencies. With stimulus levels expressed in sensation level (i.e., dB above threshold, dB SL) latency differences between Nf2 cKO+ND1 and control groups were reduced such that there were no significant differences found. This indicates that changes in vestibular sensitivity contributed to the differences in latencies seen at +6 dB re:1g/ms. f,g) Normalized VsEP amplitudes. Stimulus level is represented as dB above threshold (dB SL). Amplitudes for the Nf2 cKO group (*) remained below those of the control and Nf2 cKO+ND1 animals for p2-n1 at the highest stimulus level (MANOVA

post hoc Bonf p2-n1 at 13 dB SL: p = 0.032). p1-n1 amplitudes at the highest stimulus level were different between the Nf2 cKO and Nf2 cKO+ND1 groups (MANOVA, post hoc Bonf., p = 0.04). See Supplemental Tables 1 and 2 for details.

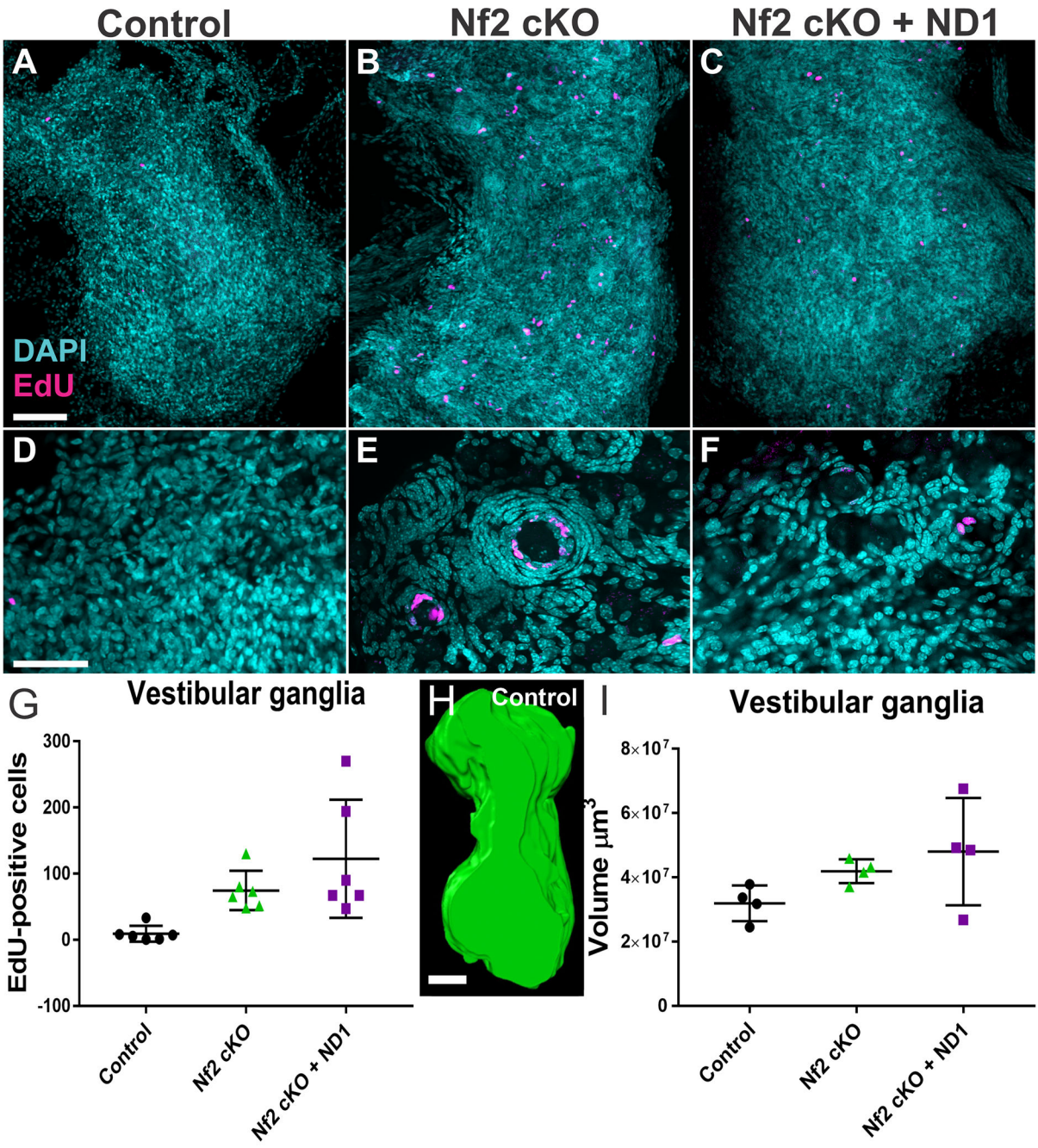

Figure 6.

Glial cell proliferation in control mice, mice with Nf2 cKO, and mice with Nf2 cKO+ND1. EdU uptake in adult mice aged 10–15 months was analyzed. Mice were injected with EdU (50mg/kg IP four times in a 24 hour period; 0, 4, 8 and 24hrs) and vestibular and geniculate ganglia were dissected within 72 hrs. EdU was detected in whole ganglion using the Click-It reaction and counterstained with DAPI. Ganglia were imaged with confocal microscopy and EdU quantified using the maximum projection of the z-stack. N=6 for each group. While only occasional spontaneous proliferations were found in control animals (A), both

vestibular and geniculate intraganglionic glia cells showed a significant increase in proliferation that was not diminished by expression of Neurod1 (B,C). Details show that the proliferation in Nf2 cKO mice primarily occurs as an aggregation of flattened nuclei around a central neuron with the distribution of EdU positive cells nearest the neuron (E,F). Note that most Nf2 mutants had an abundance of these nodules which were nearly absent in control ganglia (D) and were smaller and fewer in Nf2 cKO+ND1 mice (compare B,C). Quantification of all EdU positive profiles in the entire vestibular and geniculate ganglia showed a clear difference between control and mutant mice (symbols reflect individual mice, vertical bar indicates standard deviation). While both Nf2 cKO and Nf2 cKO+ND1 mice had elevated levels of EdU compared to control, the latter group had the widest range of EdU positive cells that is in part related to overall size differences.

Effects of Neurod1 Expression on Mouse and Human Schwannoma Cells

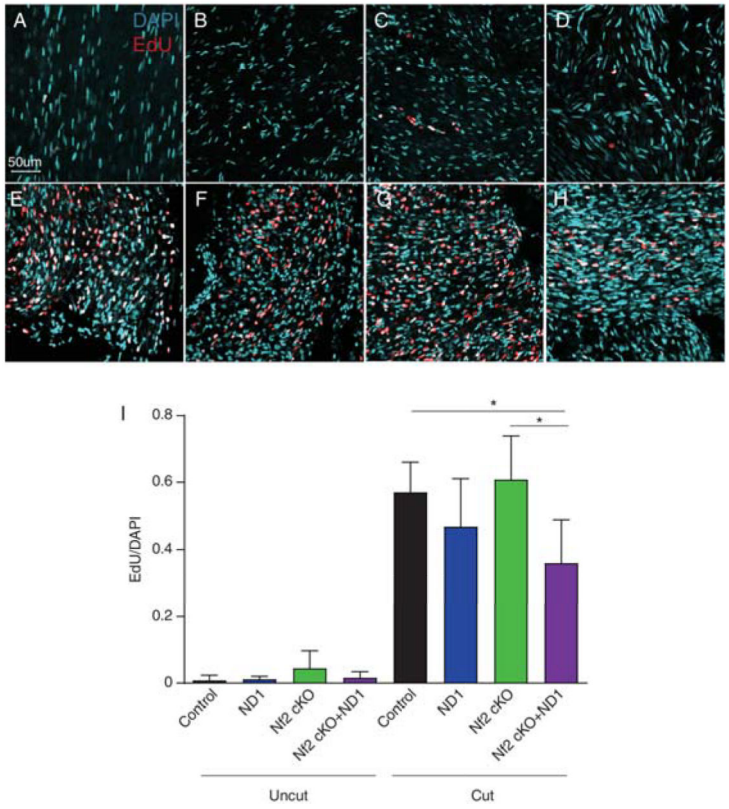

Figure 7.

Effect of cutting the sciatic nerve of various mouse mutants on EdU incorporation. Only Nf2 control (uncut) nerves show noticeable EdU incorporation consistent with Nf2 mediated Schwann cell proliferation (A-D). All cut nerves showed expected increase in proliferation as revealed with EdU uptake (E-H). However, while ND1 expression alone had only minor effects on proliferation, there was a significant decrease in proliferation in Nf2 cKO+ND1 nerves compared to NF2 cKO and control animals (*p<0.01) (I). N=6 control, N=4 Postn-Cre+ND1 (ND1), N=5 Nf2 cKO, N=5 Nf2 cKO+ND1